INTERNATIONAL JOURNAL FOR NUMERICAL METHODS IN ENGINEERING, VOL. 28, 2275–2292 (1989)

A PLATE BENDING ELEMENT BASED ON A GENERALIZED LAMINATE PLATE THEORY

J. N. REDDY* AND E. J. BARBERO†

Department of Engineering Science and Mechanics, Virginia Polytechnic Institute and State University, Blacksburg, VA 24061, U.S.A.

J. L. TEPLY‡

Alcoa Technical Center, Alcoa Center, PA 15069, U.S.A.

SUMMARY

A plate bending element based on the generalized laminate plate theory (GLPT) developed by the senior author is described and its accuracy is investigated by comparison with the exact solutions of the generalized plate theory and the 3D-elasticity theory. The element accounts for transverse shear deformation and layer-wise description of the inplane displacements of the laminate. The element has improved description of the inplane as well as the transverse deformation response. A method for the computation of interlaminar (transverse) stresses is also presented.

1. BACKGROUND

Laminated composite plates are often modelled using the classical laminate plate theory (CLPT) or the first-order shear deformation plate theory (FSDT). In both cases the laminate is treated as a single-layer plate with equivalent stiffnesses, and the displacements are assumed to vary through the thickness according to a single expression (see Reddy[1]), not allowing for possible discontinuities in strains at an interface of dissimilar material layers.

Recently, Reddy[2] presented a general laminate plate theory that allows layer-wise representation of inplane displacements, and an improved response of inplane and transverse shear deformations is predicted. Similar but different theories have appeared in the literature.[3–6] In the generalized laminate plate theory (GLPT) the equations of three-dimensional elasticity are reduced to differential equations in terms of unknown functions in two dimensions by assuming layer-wise approximation of the displacements through the thickness. Consequently, the strains are different in different layers. Exact analytical solutions of the theory were developed by the authors[7,8] to evaluate the accuracy of the theory compared to the 3D-elasticity theory. The results indicated that the generalized laminate plate theory allows accurate determination of interlaminar stresses.

The present study deals with the finite-element formulation of the theory and its application to laminated composite plates. In the interest of brevity only the main equations of the theory are reviewed and the major steps of the formulation are presented. The accuracy of the numerical

*Clifton C. Garvin Professor
†Graduate Research Assistant
‡Senior Technical Specialist

0029–5981/89/112275–18$09.00

Received 26 July 1988
Revised 3 March 1989

results obtained using the present plate element is discussed in light of the exact solutions of the theory.

2. A REVIEW OF GLPT

Consider a laminated plate composed of N orthotropic lamina, each being oriented arbitrarily with respect to the laminate (x, y) co-ordinates, which are taken to be in the midplane of the laminate. The displacements (u_1, u_2, u_3) at a point (x, y, z) in the laminate are assumed to be of the form[2]

$$\begin{aligned} u_1(x, y, z) &= u(x, y) + U(x, y, z) \\ u_2(x, y, z) &= v(x, y) + V(x, y, z) \\ u_3(x, y, z) &= w(x, y) \end{aligned} \tag{1}$$

where (u, v, w) are the displacements of a point $(x, y, 0)$ on the reference plane of the laminate, and U and V are functions which vanish on the reference plane:

$$U(x, y, 0) = V(x, y, 0) = 0 \tag{2}$$

The reference plane is taken to be the midplane of the laminate. In equation (1) the transverse deflection is restricted to be constant through the laminate thickness. This restriction is commonly used both in classical and shear deformation theories, and it can be removed if desired.

The three-dimensional theory is reduced to a two-dimensional one by assuming that U and V vary according to the expressions

$$\begin{aligned} U(x, y, z) &= \sum_{J=1}^{N} U_J(x, y)\Psi^J(z) \\ V(x, y, z) &= \sum_{J=1}^{N} V_J(x, y)\Psi^J(z) \end{aligned} \tag{3}$$

where U_J and V_J are undetermined coefficients and Ψ^J are any continuous functions that satisfy the condition

$$\Psi^J(0) = 0 \quad \text{for all } J = 1, 2, \ldots, N \tag{4}$$

The approximation in equation (3) can also be viewed as the global semi-discrete finite-element approximations of U and V through thickness. In that case Ψ^J denote the global interpolation functions, and U_J and V_J are the global nodal values of U and V at the nodes through the thickness of the laminate. For example, a finite-element approximation based on the Lagrangian interpolation through thickness can be obtained from equation (3) by setting (if the midplane does not coincide with an interface, it is used as an interface to satisfy equation (2)) $N = pn + 1$, where

n = number of subdivisions through the thickness,
p = degree of the global interpolation polynomials, $\Psi^J(z)$,
and
U_J, V_J = global nodal values of U and V (5a)

For example, if a piecewise linear displacement distribution is chosen, the corresponding functions $\Psi^J(z)$ are

$$\Psi^J(z) = \begin{cases} \dfrac{z - z_{J-1}}{z_J - z_{J-1}}; & z_{J-1} < z < z_J \\ \dfrac{z_{J+1} - z}{z_{J+1} - z_J}; & z_J < z < z_{J+1} \end{cases} \tag{5b}$$

where z_J denote the global thickness co-ordinate of the node between the Jth and $(J+1)$st subdivisions. In this case, the present theory is a layer-wise first-order shear deformation theory, but allows an accurate representation of a laminate behaviour.

Note that the number of subdivisions (or finite elements) n through the thickness can be, in principle, less than, equal to or greater than the number of layers in the laminate. When n is less than the number of layers, it amounts to modelling the total laminate as a collection of sublaminates. In the present study, n is taken equal to the number of layers.

The equilibrium equations of the theory can be derived using the principle of virtual displacements[1,2]

$$0 = \int_\Omega \left\{ N_x\left(\frac{\partial \delta u}{\partial x}\right) + N_y\left(\frac{\partial \delta v}{\partial y}\right) + N_{xy}\left(\frac{\partial \delta u}{\partial y} + \frac{\partial \delta v}{\partial x}\right) + Q_x\frac{\partial \delta w}{\partial x} + Q_y\frac{\partial \delta w}{\partial y} + \sum_{J=1}^{N}\left[N_x^J\frac{\partial \delta U_J}{\partial x} + N_y^J\frac{\partial \delta V_J}{\partial y} + N_{xy}^J\left(\frac{\partial \delta U_J}{\partial y} + \frac{\partial \delta V_J}{\partial x}\right) + Q_x^J U_J + Q_y^J V_J\right] - q\delta w \right\} \mathrm{d}A \tag{6a}$$

where

$$\begin{aligned} (N_x, N_y, N_{xy}) &= \int_{-h/2}^{h/2} (\sigma_x, \sigma_y, \sigma_{xy})\,\mathrm{d}z \\ (Q_x, Q_y) &= \int_{-h/2}^{h/2} (\sigma_{xz}, \sigma_{yz})\,\mathrm{d}z \\ (N_x^J, N_y^J, N_{xy}^J) &= \int_{-h/2}^{h/2} (\sigma_x, \sigma_y, \sigma_{xy})\,\Psi^J(z)\,\mathrm{d}z \\ (Q_x^J, Q_y^J) &= \int_{-h/2}^{h/2} (\sigma_{xz}, \sigma_{yz})\frac{\mathrm{d}\Psi^J(z)}{\mathrm{d}z}\,\mathrm{d}z \end{aligned} \tag{6b}$$

$(\sigma_x, \sigma_y, \sigma_{xy}, \sigma_{xz}, \sigma_{yz})$ are the stresses and q is the distributed transverse load. The virtual work statement in equation (6a) gives $2N+3$ differential equations in $(2N+3)$ variables (u, v, w, U_J, V_J). The form of the geometric and force boundary conditions is given in Table I. Here (n_x, n_y) denote the direction cosines of a unit normal to the boundary of the midplane Ω.

Table I

Geometric (essential)	Force (natural)
u	$N_x n_x + N_{xy} n_y$
v	$N_{xy} n_x + N_y n_y$
w	$Q_x n_x + Q_y n_y$
U_J	$N_x^J n_x + N_{xy}^J n_y$
V_J	$N_{xy}^J n_x + N_y^J n_y$

(7)

The constitutive equations of the laminate are given by

$$\{N\} = [A]\{e\} + \sum_{K=1}^{N} [B_K]\{e_K\} \tag{8a}$$

$$\{N^J\} = [B^J]\{e\} + \sum_{K=1}^{N} [D^{JK}]\{e_K\} \tag{8b}$$

where the strains $\{e\}$ and $\{e_K\}$, and the matrices $[A]$, $[B_J]$ and $[D^{JK}]$ are given in Reference 2; also see Appendix I.

3. ANALYTICAL SOLUTION

Consider a rectangular ($a \times b$) cross-ply laminate, not necessarily symmetric, composed of N layers. For such a laminate the constitutive equations (8) simplify because $A_{16} = A_{26} = A_{45} = B_{16}^K = B_{26}^K = B_{45}^K = D_{16}^{JK} = D_{26}^{JK} = D_{45}^{JK} = 0$. The governing equations become

$$
\begin{aligned}
&A_{11}u_{,xx} + A_{12}v_{,yx} + A_{66}(u_{,yy} + v_{,xy}) \\
&\qquad + \sum_{K=1}^{N} [B_{11}^K U_{K,xx} + B_{12}^K V_{K,yx} + B_{66}^K (U_{K,yy} + V_{K,xy})] = 0 \\
&A_{66}(u_{,yx} + v_{,xx}) + A_{12}u_{,xy} + A_{22}v_{,yy} \\
&\qquad + \sum_{K=1}^{N} [B_{66}^K (U_{K,yx} + V_{K,xx}) + B_{12}^K U_{K,xy} + B_{22}^K V_{K,yy}] = 0 \\
&A_{55}w_{,xx} + A_{44}w_{,yy} + \sum_{K=1}^{N} [B_{55}^K U_{K,x} + B_{44}^K V_{K,y}] + q = 0 \\
&B_{11}^J u_{,xx} + B_{12}^J v_{,yx} + B_{66}^J (v_{,yy} + v_{,xy}) - B_{55}^J w_{,x} \\
&\qquad + \sum_{K=1}^{N} [D_{11}^{JK} U_{K,xx} + D_{12}^{JK} V_{K,yx} + D_{66}^{JK} (U_{K,yy} + V_{K,xy}) - D_{55}^{JK} U_K] = 0 \\
&B_{66}^J (u_{,yx} + v_{,xx}) + B_{12}^J u_{,xy} + B_{22}^J v_{,yy} - B_{44}^J w_{,y} \\
&\qquad + \sum_{K=1}^{N} [D_{66}^{JK} (U_{K,yx} + V_{K,xx}) + D_{12}^{JK} U_{K,xy} + D_{22}^{JK} V_{K,yy} - D_{44}^{JK} V_K] = 0
\end{aligned}
\tag{9}
$$

for $I, J = 1, 2, \ldots, N$.

Here we consider the Navier solution[1,7,8] of the above equations for the simply supported boundary conditions:

$$
\begin{aligned}
&v = w = V_K = N_x = N_x^K = 0; \quad x = 0, a; \quad k = 1, \ldots, N \\
&u = w = U_K = N_y = N_y^K = 0; \quad y = 0, b; \quad k = 1, \ldots, N
\end{aligned}
\tag{10}
$$

These boundary conditions are identically satisfied by the following expressions for displacements:

$$
\begin{aligned}
u &= \sum_{m,n}^{\infty} X_{mn} \cos \alpha x \sin \beta y \\
v &= \sum_{m,n}^{\infty} Y_{mn} \sin \alpha x \cos \beta y \\
w &= \sum_{m,n}^{\infty} W_{mn} \sin \alpha x \sin \beta y \\
U_k &= \sum_{m,n}^{\infty} R_{mn}^k \cos \alpha x \sin \beta y \\
V_k &= \sum_{m,n}^{\infty} S_{mn}^k \sin \alpha x \cos \beta y
\end{aligned}
\tag{11}
$$

where

$$\alpha = \frac{m\pi}{a}; \quad \beta = \frac{n\pi}{b}; \quad k = 1, \ldots, N$$

The transverse distributed load can also be expanded in double Fourier series as

$$q(x, y) = \sum_{m,n}^{\infty} q_{mn} \sin \alpha x \sin \beta y \tag{12}$$

Substitution of these expressions into the governing equations gives a system of $2N + 3$ equations for each of the Fourier modes (m, n), from which we obtain the coefficients $(X_{mn}, Y_{mn}, W_{mn}, R^k_{mn}, S^k_{mn})$:

$$\begin{bmatrix} [C] & [C^J] \\ [C^J]^T & [C^{JK}] \end{bmatrix} \begin{Bmatrix} \{\Delta^1\} \\ \{\Delta^2\} \end{Bmatrix} = \begin{Bmatrix} 0 \\ 0 \\ q_{mn} \\ 0 \end{Bmatrix} \tag{13}$$

where $\{\Delta^1\}^T = \{X_{mn}, Y_{mn}, W_{mn}\}$, $\{\Delta^2\}^T = \{R^k_{mn}, S^k_{mn}\}$, and the coefficient matrices $[C]$, $[C^J]$ and $[C^{JK}]$ are given in Appendix I. Once the coefficients $(X_{mn}, Y_{mn}, W_{mn}, R^k_{mn}, S^k_{mn})$ are obtained, the stresses can be computed using equation (8).

4. FINITE-ELEMENT FORMULATION

The generalized displacements (u, v, w, U_J, V_J) are expressed, over each element, as a linear combination of the two-dimensional interpolation functions ψ_i and the nodal values $(u^i, v^i, w^i, U^i_J, V^i_J)$ as follows:

$$(u, v, w, U_J, V_J) = \sum_{i=1}^{m} (u^i, v^i, w^i, U^i_J, V^i_J)\psi_i \tag{14}$$

where m is the number of nodes per element.

Using equation (14), the strains can be expressed in the form

$$\{e\} = [H]\{\Delta\}, \qquad \{e_J\} = [\bar{H}]\{\Delta_J\} \tag{15a}$$

where

$$\{\Delta\} = \begin{Bmatrix} \{u\} \\ \{v\} \\ \{w\} \end{Bmatrix}, \qquad \{\Delta_J\} = \begin{Bmatrix} \{U_J\} \\ \{V_J\} \end{Bmatrix} \tag{15b}$$

The matrices $[H]$ and $[\bar{H}]$ are given in Appendix I.

Using equations (14) in the virtual work statement (6a), we obtain the finite-element model

$$\begin{bmatrix} [H]^T[A][H] & [H]^T[B^1][\bar{H}] & \cdots & [H]^T[B^N][\bar{H}] \\ [\bar{H}][B^1][H]^T & [\bar{H}]^T[D^{11}][\bar{H}] & \cdots & \cdot \\ \cdot & & \cdots & \cdot \\ \cdot & & \cdots & \cdot \\ [\bar{H}][B^N][H]^T & & \cdots & [\bar{H}]^T[D^{NN}][\bar{H}] \end{bmatrix} \begin{Bmatrix} \{\Delta\} \\ \{\Delta_1\} \\ \cdot \\ \cdot \\ \{\Delta_N\} \end{Bmatrix} = \begin{Bmatrix} \{q\} \\ \{0\} \\ 0 \\ 0 \\ \{0\} \end{Bmatrix} \tag{16}$$

For piecewise linear interpolation of U and V through the thickness, $[H]$ is a 5 by 3 matrix and $[\bar{H}]$ is a 5 by 2 matrix.

5. INTERLAMINAR STRESS CALCULATION

When a piecewise linear interpolation through the thickness is used, GLPT provides an excellent representation of the displacements, and accurate prediction of the inplane stresses (σ_{xx}, σ_{yy}, σ_{xy}), as was demonstrated in References 7 and 8. Interlaminar stresses (σ_{xz}, σ_{yz}, σ_{zz}) can be computed, as was done in Reference 8, from the equilibrium equations of 3D-elasticity when exact analytical solutions are available. An approximate technique is used in this study to integrate the equilibrium equations, using the inplane stress information provided by the finite element solution. The scheme as presented in Reference 9 is extended here to quadrilateral isoparametric elements. It approximates the shear stress distribution through each layer with a quadratic function, thus requiring $3n$ equations for each of the shear stresses (σ_{xz}, σ_{yz}), where n is the number of layers; n equations are used to satisfy the n average shear stresses on each layer. Two equations are used to impose vanishing shear stresses at the surfaces of the plate. Then, $(n-1)$ equations are employed to satisfy continuity of the shear stresses at the interfaces between layers. Finally, the remaining $(n-1)$ equations are used to compute the jump in $\sigma_{xz,z}$ (or $\sigma_{yz,z}$) at each interface.

The average shear stresses on each layer are computed from the constitutive equations and the displacement field obtained in the finite-element analysis.

In this work, unlike Reference 8, the following equilibrium equations

$$\begin{aligned} \sigma_{xz,z} &= -(\sigma_{xx,x} + \sigma_{xy,y}) \\ \sigma_{yz,z} &= -(\sigma_{xy,x} + \sigma_{yy,y}) \end{aligned} \tag{17}$$

are used to compute $\sigma_{xz,z}$ and $\sigma_{yz,z}$ directly from the finite-element approximation. The inplane components of the stresses and their inplane derivatives ($\sigma_{xx,x}$; $\sigma_{yy,y}$; $\sigma_{xy,x}$ and $\sigma_{xy,y}$) are computed from the constitutive equations for each layer, i.e.

$$\begin{Bmatrix} \sigma_x \\ \sigma_y \\ \sigma_{xy} \end{Bmatrix} = \begin{bmatrix} Q_{11} & Q_{12} & Q_{13} \\ Q_{12} & Q_{22} & Q_{23} \\ Q_{13} & Q_{23} & Q_{33} \end{bmatrix} \begin{Bmatrix} \dfrac{\partial u}{\partial x} + \displaystyle\sum_{J=1}^{N} \dfrac{\partial U_J}{\partial x}\Psi^J \\ \dfrac{\partial v}{\partial x} + \displaystyle\sum_{J=1}^{N} \dfrac{\partial V_J}{\partial x}\Psi^J \\ \dfrac{\partial u}{\partial y} + \dfrac{\partial v}{\partial x} + \displaystyle\sum_{J=1}^{N} \left(\dfrac{\partial U_J}{\partial y} + \dfrac{\partial V_J}{\partial x}\right)\Psi^J \end{Bmatrix} \tag{18}$$

The procedure thus requires computation of second derivatives of the displacements (u, v, U_J, V_J) (see Reference 10, p. 7-2-11, pp. 435), as presented in Appendix II.

6. NUMERICAL EXAMPLES

Several numerical examples are presented to assess the quality of the finite-element model and to display the features of the GLPT in the modelling of laminated composite plates. Whenever possible, comparison is made with 3D-elasticity solutions. Two problems of bending of composite laminates that can be analytically solved using the full 3D-elasticity equations are the cylindrical bending of cross-ply plates and the bending of simply supported plates. The cylindrical bending problem is one in which one of the planar dimensions of the plate is much larger (in theory, of infinite length along the y-axis) than the other. The generalized plane-strain conditions previal, and it is sufficient to consider only a unit width along the y-axis. The problem is then reduced to a one-dimensional beam problem. Only certain symmetric laminates can be analysed in cylindrical bending because other lamination schemes would violate the generalized plane-strain condition.

Analytical solutions to the 3D-equations of elasticity for cylindrical bending exist for simply supported boundary conditions.[11] Analytical solutions to the 3D-equations of elasticity for square plate also exist for simply supported, cross-ply laminates.[12] For more general cases that do not admit analytical solutions to the 3D-elasticity equations we can still compare the finite-element solutions to closed-form solutions of GLPT. Navier type solutions were presented in References 7 and 8 for square plates and cylindrical bending. Since the Navier technique is restricted to simply supported boundary conditions, the authors developed closed-form solutions for cylindrical bending (using eigenvalue expansions[7,8]) that admit any combination of boundary conditions. Comparisons to other theories like the classical laminated plate theory[1] are presented to demonstrate the accuracy of the new theory.

6.1. *Cylindrical bending of a (0/90) plate strip*

Transverse deflections, normalized with respect to the classical laminated plate theory solution, are plotted in Figure 1 for a (0/90) laminated plate in cylindrical bending. The material properties used are those of graphite-epoxy:

$$\begin{aligned} &E_1 = 19{\cdot}2 \times 10^6 \text{ psi}, \quad E_2 = 1{\cdot}56 \times 10^6 \text{ psi} \\ &G_{12} = G_{13} = 0{\cdot}82 \times 10^6 \text{ psi} \\ &G_{23} = 0{\cdot}523 \times 10 \text{ psi}, \quad \nu_{12} = \nu_{13} = 0{\cdot}24 \\ &\nu_{23} = 0{\cdot}49 \end{aligned} \tag{19}$$

A uniform load and three different boundary conditions were used (SS = simply supported at both ends, CC = clamped at both ends and CT = cantilever). The 3D-elasticity solution[10] for the simply supported case and the closed-form solutions of GLPT[7,8] for the three types of boundary conditions are plotted for comparison. Five elements were used to represent one-half of the plate for the SS and CC cases, taking advantage of the symmetry of the problem; and 10 elements are used for the CT case, which has no symmetry. Very good agreement is found between the finite-element solution and the exact solutions.

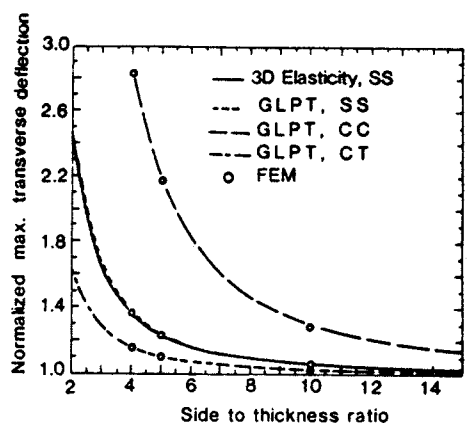

Figure 1. Comparison between the 3D analytical solution, GLPT analytical solutions and GLPT finite-element solutions for a (0/90) laminated plate in cylindrical bending. The transverse load is uniformly distributed and three boundary conditions (SS = simply supported, CC = clamped and CT = cantilever) are considered

6.2. *Cylindrical bending of a (0/90/0) plate strip*

A long, (0/90/0) laminated plate ($a/h = 4$), simply supported along the long edges and subjected to sinusoidal load, is analysed. The plate can be analysed using any strip along the length. The underlying assumption is that every line along the length deforms into the same shape (called cylindrical bending). The problem becomes essentially one-dimensional (e.g. a beam).

The material properties used are

$$\begin{aligned} E_1 &= 25 \times 10^5 \text{ psi}, \quad E_2 = 10^6 \text{ psi} \\ G_{12} &= G_{13} = 0{\cdot}5 \times 10^6 \text{ psi} \\ G_{23} &= 0{\cdot}2 \times 10^6 \text{ psi}, \quad \nu_{12} = \nu_{13} = \nu_{23} = 0{\cdot}25 \end{aligned} \tag{20}$$

The displacements and stresses are normalized as follows:

$$\begin{aligned} \bar{u} &= \frac{100E_2}{q_0 h s^3} u, \qquad \bar{w} = \frac{100E_2}{q_0 h s^4} w \\ \bar{\sigma}_{xz} &= \frac{1}{s q_0} \sigma_{xz}, \qquad \bar{\sigma}_{xx} = \frac{1}{s^2 q_0} \sigma_{xx} \end{aligned} \tag{21}$$

where $s = a/h$, a = width and h = total thickness of the plate. Both one-dimensional and two-dimensional elements were used in this example, imposing the appropriate boundary conditions on the plate elements to simulate the generalized plane-strain (i.e. cylindrical bending) condition. Under these conditions, both elements gave exactly the same results.

Eight four-node linear elements were used to represent one-half of the span. Comparisons with the 3D-elasticity solution are made in Figures 2 to 4. Through-the-thickness distributions of the inplane displacements u obtained by various theories are shown in Figure 2. The GLPT solution is in excellent agreement with the 3D-elasticity solution, whereas the CLPT solution is in considerable error. The inplane normal stress σ_{xx} computed in the CLPT (see Figure 3) differs even in sign at the interface of laminae.

Eight nine-node quadratic elements are used to obtain the through-the-thickness distribution of shear stress σ_{xz} from the equilibrium equations, and the result is shown in Figure 4. Note that the 3D-elasticity solution is slightly unsymmetric because the load applied at the top surface is

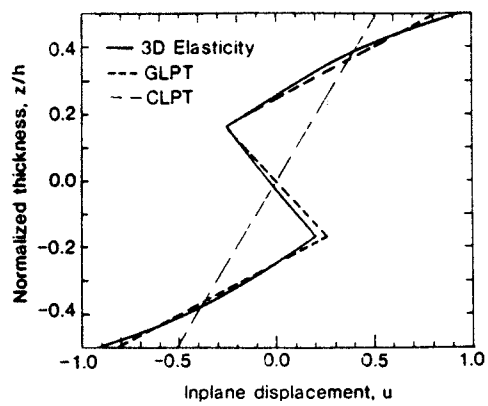

Figure 2. Through-the-thickness distribution of the inplane displacement u for a simply supported (0/90/0) laminate under sinusoidal load, $a/h = 4$

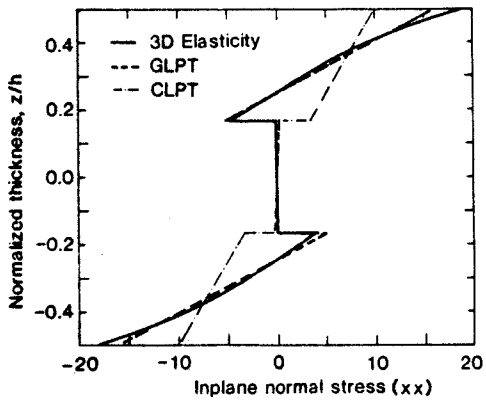

Figure 3. Through-the thickness distribution of the inplane normal stress σ_{xx} for a simply supported (0/90/0) laminate under sinusoidal load, $a/h = 4$

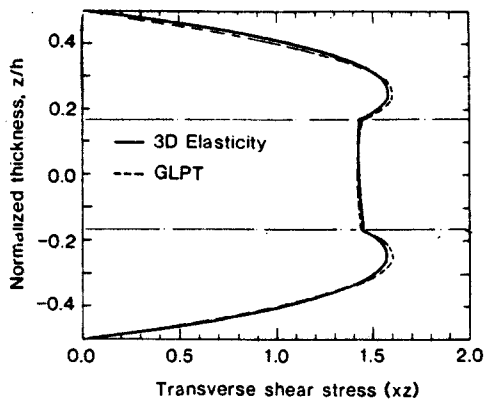

Figure 4. Through-the-thickness distribution of the transverse shear stress σ_{xz} for a simply supported (0/90/0) laminate under sinusoidal load, $a/h = 4$

unsymmetric about the midplane, while the GLPT solution is symmetric because it is assumed to be applied at the midplane, as is the case with all plate theories.

6.3. Simply supported square laminate (0/90/0) under sinusoidal load

This example is chosen because there exists an exact 3D-elasticity solution.[11] The material properties used are the same as those used in Section 6.2. Owing to symmetry (geometric as well as material), only one quarter of the laminate is modelled using a 4 × 4 uniform mesh of quadratic elements. A co-ordinate system with the origin at the centre of the plate is used for reference. The simply supported boundary conditions used are the same as those used to obtain the 3D-elasticity solution:

$$w = u = U_J = 0 \quad \text{at} \quad y = \pm a/2$$

$$w = v = V_J = 0 \quad \text{at} \quad x = \pm a/2$$

The following normalizations of stresses are used in presenting the results:

$$(\bar{u}, \bar{v}) = \frac{100E_2}{q_0 hs^3}(u, v), \qquad \bar{w} = \frac{100E_2}{q_0 hs^4}w, \qquad (\bar{\sigma}_{xz}, \bar{\sigma}_{yz}) = \frac{1}{q_0 s}(\sigma_{xz}, \sigma_{yz})$$
$$(\bar{\sigma}_{xx}, \bar{\sigma}_{yy}, \bar{\sigma}_{xy}) = \frac{1}{q_0 s^2}(\sigma_{xx}, \sigma_{yy}, \sigma_{xy}) \tag{22}$$

where $s = a/h$, a is the length of the square plate and h is the thickness of the plate. The stresses were computed at the following locations, which are the centre points of the elements:

$$\sigma_{xx}\left(\frac{a}{16}, \frac{a}{16}\right), \quad \sigma_{yy}\left(\frac{a}{16}, \frac{a}{16}\right) \quad \text{and} \quad \sigma_{xy}\left(\frac{7a}{16}, \frac{7a}{16}\right) \tag{23}$$

The stress distributions through laminate thickness are shown in Figures 5 to 7 for $s = 4$. The quality of the GLPT solution and the accuracy of the finite-element solutions are apparent from the figures.

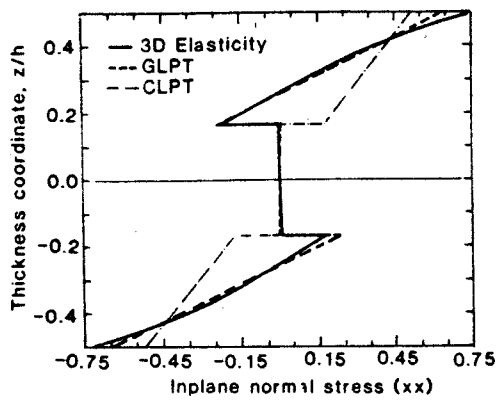

Figure 5. Through-the-thickness distribution of the inplane normal stress σ_{xx} for a simply supported (0/90/0) laminated square plate under double-sinusoidal load, $a/h = 4$

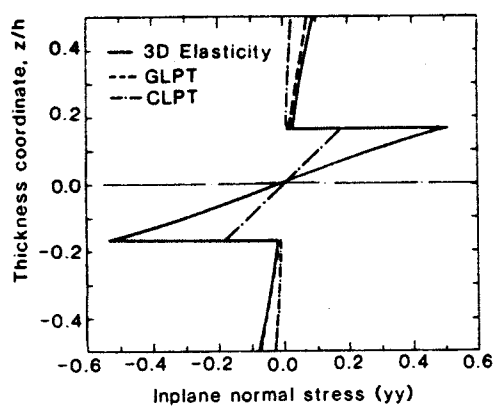

Figure 6. Through-the-thickness distribution of the inplane normal stress σ_{yy} for a simply supported (0/90/0) laminated square plate under double-sinusoidal load, $a/h = 4$

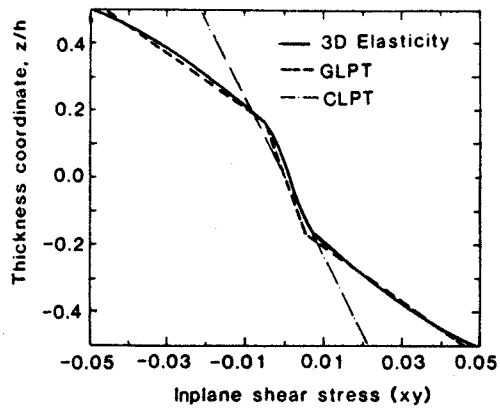

Figure 7. Through-the-thickness distribution of the inplane shear stress σ_{xy} for a simply supported (0/90/0) laminated square plate under double-sinusoidal load, $a/h = 4$

6.4. *Simply supported (0/90/0) laminate under uniform load*

Next we consider the case of a simply supported (0/90/0) plate under uniformly distributed transverse load. The material properties used are those of a gaphite-epoxy material given in equation (14). The plate is simply supported on all four sides. Owing to symmetry, only a quarter of the plate is modelled. The appropriate boundary conditions for a simply supported cross-ply laminate, with symmetry axes along $x = 0$ and $y = 0$ are[13]

$$\begin{aligned} &\text{on } x = 0: && u = U_j = 0 \\ &\text{on } y = 0: && v = V_j = 0 \\ &\text{on } x = a: && v = w = V_j = 0 \\ &\text{on } y = b: && u = w = U_j = 0 \end{aligned} \tag{24}$$

The through-the-thickness distribution of the inplane normal stress σ_{xx}, for aspect ratio $a/h = 10$, is shown in Figure 8. The stresses were computed at the Gauss point $x = 0{\cdot}0528a$ and $y = 0{\cdot}0528a$. Figures 9 and 10 contain similar plots of the interlaminar shear stresses σ_{yz} and σ_{xz}, respectively. In Figure 9 σ_{yz} is computed at the point $x = 0{\cdot}0528a$ and $y = 0{\cdot}9472a$, in Figure 10 σ_{xz} is computed at the point $x = 0{\cdot}9472a$ and $y = 0{\cdot}0528a$. In these plots, broken lines represent stresses obtained from the constitutive equations, while the smooth solid line represents the stress distribution obtained using the equilibrium equations. Stresses obtained using the GLPT and FSDT are compared in these figures. In this case, the GLPT admits analytic solution; the finite-element solution agrees with the analytical solution. The stress components predicted by the GLPT are in close agreement with the 3D-elasticity solution. The differences between the stresses computed in the FSDT and GLPT theories are significant for $a/h = 10$, but the difference reduces as the a/h ratio increases.

6.5. *Simply supported (45/−45/45/−45) laminate under uniform load*

While the inplane stresses obtained using FSDT and GLPT in a cross-ply plate are reasonably close, the stresses differ significantly for an antisymmetric angle-ply laminate. This is illustrated in

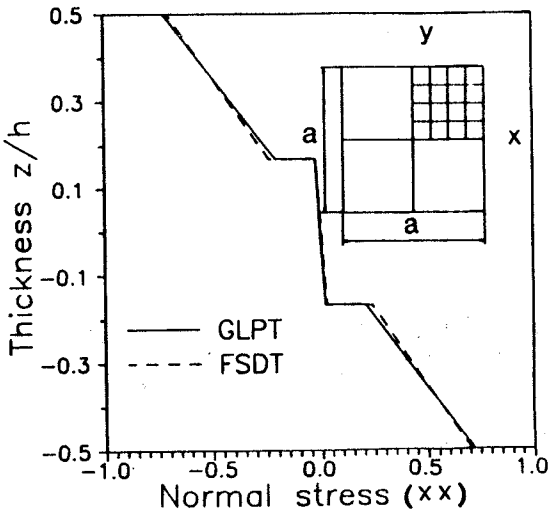

Figure 8. Through-the-thickness distribution of the inplane normal stress σ_{xx} for a simply supported (0/90/0) laminated square plate under uniform load, $(a/h = 10)$ as computed using GLPT and FSDT

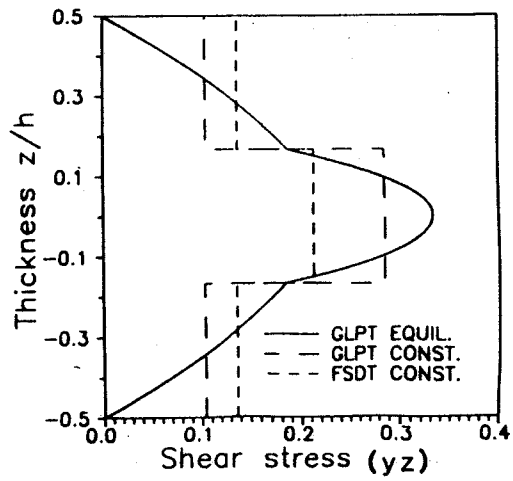

Figure 9. Through-the-thickness distribution of the transverse shear stress σ_{yz} for a simply supported (0/90/0) laminated square plate under uniform load, $(a/h = 10)$ as computed using GLPT and FSDT

this example. Consider the case of an antisymmetric angle-ply $(45/-45/45/-45)$ plate under uniformly distributed transverse load. The material properties are the same as those in the previous example.

The plate is simply supported on all four sides. Owing to symmetry only a quarter of the plate is modelled. The appropriate boundary conditions for a simply supported antisymmetric angle-ply rectangular laminate, with symmetry axes at $x = 0$ and $y = 0$ are[13]

$$\begin{aligned} &\text{on } x = 0: && v = U_j = 0 \\ &\text{on } y = 0: && u = V_j = 0 \\ &\text{on } x = a: && v = w = V_j = 0 \\ &\text{on } y = b: && u = w = U_j = 0 \end{aligned} \tag{25}$$

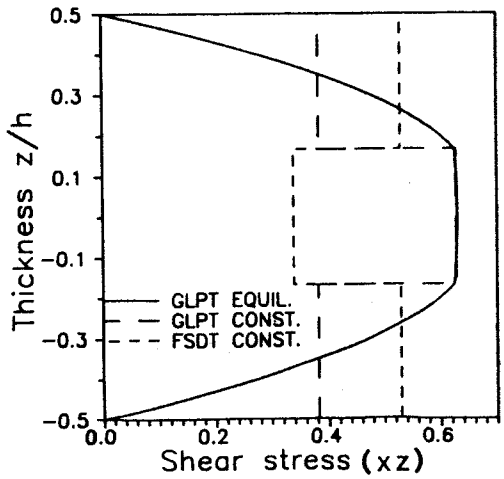

Figure 10. Through-the-thickness distribution of the transverse shear stress σ_{xz} for a simply supported (0/90/0) laminated square plate under uniform load, $(a/h = 10)$ as computed using GLPT and FSDT

Figures 11 and 12 contain plots of through-the-thickness distribution of the inplane stresses σ_{xx} and σ_{xy}, respectively, for aspect ratio $a/h = 10$. Both figures correspond to the Gauss point $x = y = 0{\cdot}0528a$. The shear correction factors used for the FSDT and GLPT are 1·0. The difference between the stresses computed by the FSDT and GLPT still persist, however reduced, even for thin laminates. For example, Figure 13 contains a plot of σ_{xx} for aspect ratio $a/h = 50$.

Figures 14 and 15 contain plots of σ_{xz} through the thickness of the same laminate at $x = 0{\cdot}9472a$, $y = 0{\cdot}0528a$ for aspect ratios of 10 and 100. The results show striking differences between FSDT and GLPT. The difference does not vanish as the aspect ratio grows. It can be seen that the non-dimensional shear stress distribution predicted by the FSDT remains almost unchanged as the aspect ratio is changed from 10 to 100. The reason for the difference can be attributed to the GLPT's ability to accurately predict interlaminar stresses, even at the free edge.

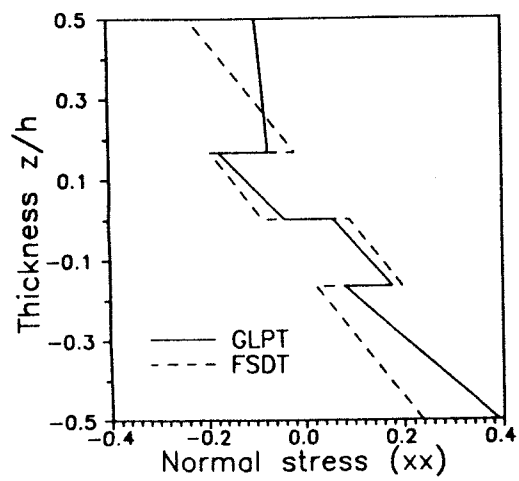

Figure 11. Through-the-thickness distribution of the stress σ_{xx} for a simply supported (45/−45/45/−45) laminated square plate under uniform load, $a/h = 10$

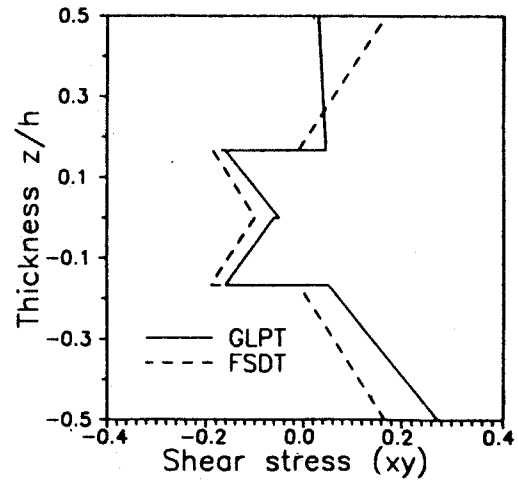

Figure 12. Through-the-thickness distribution of the stress σ_{xy} for a simply supported (45/−45/45/−45) laminated square plate under uniform load, $a/h = 10$

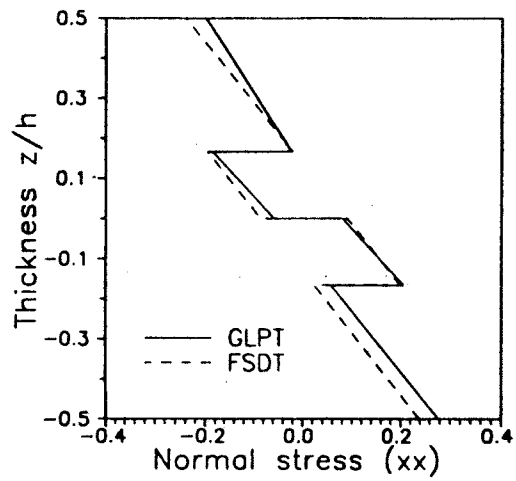

Figure 13. Through-the-thickness distribution of the inplane normal stress σ_{xx} for a simply supported (45/−45/45/−45) laminated square plate under uniform load, $a/h = 50$

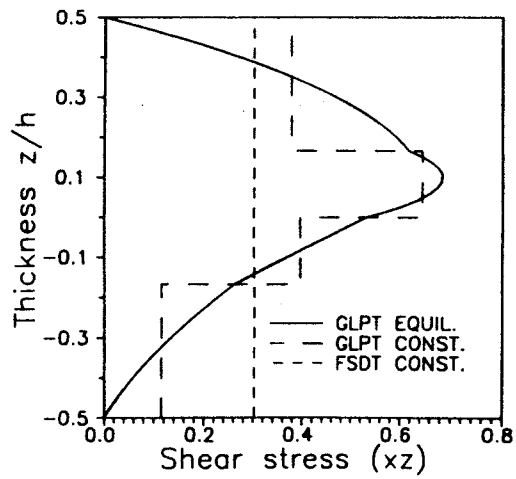

Figure 14. Through-the-thickness distribution of the transverse shear stress σ_{xz} for a simply supported (45/−45/45/−45) laminated square plate under uniform load, $a/h = 10$

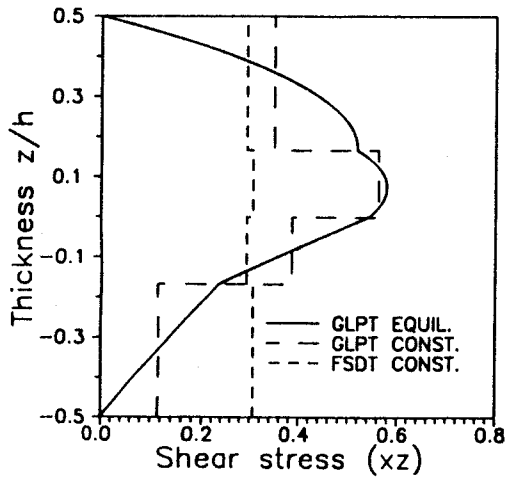

Figure 15. Through-the-thickness distribution of the transverse stress σ_{xz} for a simply supported (45/−45/45/−45) laminated square plate under uniform load, $a/h = 100$

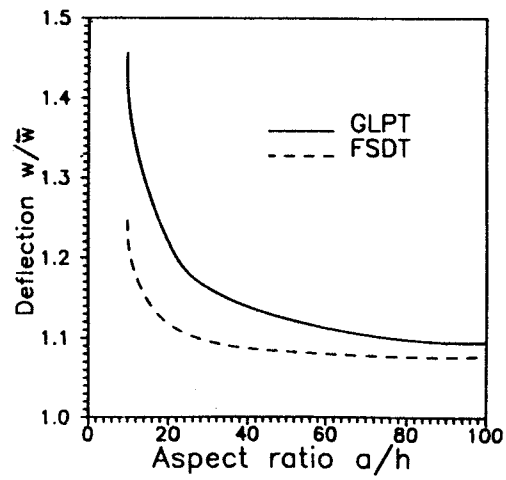

Figure 16. Normalized transverse deflection versus aspect ratio for the antisymmetric angle-ply (45/−45/45/−45) square plate under uniform load

Finally, Figure 16 contains a plot of the non-dimensional maximum transverse deflection w as a function of the aspect ratio of the plate. The difference between the two theories can be attributed to the different representation of the shear deformation. In this case the shear correction factor used in both theories is one. It is well known that the FSDT requires a shear correction factor smaller than one to produce the correct transverse deflection.

7. CONCLUSIONS

A displacement finite-element formulation of the generalized laminate plate theory of Reddy[2] is presented and the accuracy of the associated plate bending element is demonstrated using several composite plate problems. The generalized laminate theory yields accurate results for both displacements and stresses. The applicability of the GLPT element to problems with dissimilar

materials and problems without analytical solutions is demonstrated. While the GLPT plate bending element is computationally expensive compared to the FSDT plate element (or the Mindlin plate element), it yields very accurate results for *all* stresses and it is less expensive compared to a three-dimensional finite element analysis of laminated composite plates. Use of the theory for delamination and failure of composites awaits attention.

APPENDIX I. STRAIN–DISPLACEMENT MATRICES AND LAMINATE STIFFNESSES

The strains $\{e\}$ and $\{e_K\}$ appearing in equation (8) are[2]

$$\{e\}=\begin{Bmatrix} \dfrac{\partial u}{\partial x} \\ \dfrac{\partial v}{\partial y} \\ \dfrac{\partial u}{\partial y}+\dfrac{\partial v}{\partial x} \\ \dfrac{\partial w}{\partial x} \\ \dfrac{\partial w}{\partial y} \end{Bmatrix}, \qquad \{e_K\}=\begin{Bmatrix} \dfrac{\partial U_K}{\partial x} \\ \dfrac{\partial V_K}{\partial y} \\ \dfrac{\partial U_K}{\partial y}+\dfrac{\partial V_K}{\partial x} \\ U_K \\ V_K \end{Bmatrix}$$

The matrices $[H]$ and $[\bar{H}]$ appearing in the strain–displacement relations (15) are

$$[H]_{(5\times 3m)}=\begin{bmatrix} \dfrac{\partial\psi_1}{\partial x} & 0 & 0 & \dfrac{\partial\psi_2}{\partial x} & 0 & 0 & \cdots & \dfrac{\partial\psi_m}{\partial x} & 0 & 0 \\ 0 & \dfrac{\partial\psi_1}{\partial y} & 0 & 0 & \dfrac{\partial\psi_2}{\partial y} & 0 & \cdots & 0 & \dfrac{\partial\psi_m}{\partial y} & 0 \\ \dfrac{\partial\psi_1}{\partial y} & \dfrac{\partial\psi_1}{\partial x} & 0 & \dfrac{\partial\psi_2}{\partial y} & \dfrac{\partial\psi_2}{\partial x} & 0 & \cdots & \dfrac{\partial\psi_m}{\partial y} & \dfrac{\partial\psi_m}{\partial x} & 0 \\ 0 & 0 & \dfrac{\partial\psi_1}{\partial x} & 0 & 0 & \dfrac{\partial\psi_2}{\partial x} & \cdots & 0 & 0 & \dfrac{\partial\psi_m}{\partial x} \\ 0 & 0 & \dfrac{\partial\psi_1}{\partial y} & 0 & 0 & \dfrac{\partial\psi_{12}}{\partial y} & \cdots & 0 & 0 & \dfrac{\partial\psi_m}{\partial y} \end{bmatrix}$$

$$[\bar{H}]_{(5\times 2m)}=\begin{bmatrix} \dfrac{\partial\psi_1}{\partial x} & 0 & \dfrac{\partial\psi_2}{\partial x} & 0 & \cdots & \dfrac{\partial\psi_m}{\partial x} & 0 \\ 0 & \dfrac{\partial\psi_1}{\partial y} & 0 & \dfrac{\partial\psi_2}{\partial y} & \cdots & 0 & \dfrac{\partial\psi_m}{\partial y} \\ \dfrac{\partial\psi_1}{\partial y} & \dfrac{\partial\psi_1}{\partial x} & \dfrac{\partial\psi_2}{\partial y} & \dfrac{\partial\psi_2}{\partial x} & \cdots & \dfrac{\partial\psi_m}{\partial y} & \dfrac{\partial\psi_m}{\partial x} \\ \psi_1 & 0 & \psi_2 & 0 & \cdots & \psi_m & 0 \\ 0 & \psi_1 & 0 & \psi_2 & \cdots & 0 & \psi_m \end{bmatrix}$$

The laminate stiffness for the present theory are[2]

$$A_{ij} = \sum_{K=1}^{N} \int_{z_K}^{z_{K+1}} Q_{ij}^{(K)} dz \quad (i,j = 1, 2, 6, 4, 5)$$

$$B_{ij}^{J} = \sum_{K=1}^{N} \int_{z_K}^{z_{K+1}} Q_{ij}^{(K)} \Psi^J dz \quad (i,j = 1, 2, 6)$$

$$D_{ij}^{JI} = \sum_{K=1}^{N} \int_{z_K}^{z_{K+1}} Q_{ij}^{(K)} \Psi^I \Psi^J dz \quad (i,j = 1, 2, 6)$$

$$B_{ij}^{J} = \sum_{K=1}^{N} \int_{z_K}^{z_{K+1}} Q_{ij}^{(K)} \frac{d\Psi^J}{dz} dz \quad (i,j = 4, 5)$$

$$D_{ij}^{JI} = \sum_{K=1}^{N} \int_{z_K}^{z_{K+1}} Q_{ij}^{(K)} \frac{d\Psi^J}{dz} \frac{d\Psi^I}{dz} dz \quad (i,j = 4, 5)$$

APPENDIX II. COMPUTATION OF HIGHER-ORDER DERIVATIVES

As discussed in Reference 10, the computation of the second- and higher-order derivatives of the interpolation functions with respect to the global co-ordinates involves additional computations.

The first-order derivatives with respect to the global co-ordinates are related to those with respect to the local (or element) co-ordinates according to

$$\begin{Bmatrix} \frac{\partial \psi_i}{\partial x} \\ \frac{\partial \psi_i}{\partial y} \end{Bmatrix} = \begin{bmatrix} \frac{\partial x}{\partial \xi} & \frac{\partial y}{\partial \xi} \\ \frac{\partial x}{\partial \eta} & \frac{\partial y}{\partial \eta} \end{bmatrix}^{-1} \begin{Bmatrix} \frac{\partial \psi_i}{\partial \xi} \\ \frac{\partial \psi_i}{\partial \eta} \end{Bmatrix} \equiv [J]^{-1} \begin{Bmatrix} \frac{\partial \psi_i}{\partial \xi} \\ \frac{\partial \psi_i}{\partial \eta} \end{Bmatrix} \tag{A1}$$

where the Jacobian matrix $[J]$ is evaluated using the approximation of the geometry:

$$x = \sum_{j=1}^{r} x_j \phi_j(\xi, \eta)$$
$$y = \sum_{j=1}^{r} y_j \phi_j(\xi, \eta) \tag{A2}$$

where ϕ_j are the interpolation functions used for the geometry and (ξ, η) are the element natural co-ordinates. For the isoparametric formulation $r = m$ (see equation (14)) and $\phi_j = \psi_j$. The second-order derivatives of ψ_i with respect to the global co-ordinates (x, y) are given by

$$\begin{Bmatrix} \frac{\partial^2 \psi_i}{\partial x^2} \\ \frac{\partial^2 \psi_i}{\partial y^2} \\ \frac{\partial^2 \psi_i}{\partial x \partial y} \end{Bmatrix} = [J_1]^{-1} \left(\begin{Bmatrix} \frac{\partial^2 \psi_i}{\partial \xi^2} \\ \frac{\partial^2 \psi_i}{\partial \eta^2} \\ \frac{\partial^2 \psi_i}{\partial \xi \partial \eta} \end{Bmatrix} - [J_2] \begin{Bmatrix} \frac{\partial \psi_i}{\partial x} \\ \frac{\partial \psi_i}{\partial y} \end{Bmatrix} \right) \tag{A3}$$

where

$$[J_1] = \begin{bmatrix} \left(\frac{\partial x}{\partial \xi}\right)^2 & \left(\frac{\partial y}{\partial \xi}\right)^2 & 2\frac{\partial y}{\partial \xi}\frac{\partial x}{\partial \xi} \\ \left(\frac{\partial x}{\partial \eta}\right)^2 & \left(\frac{\partial y}{\partial \eta}\right)^2 & 2\frac{\partial x}{\partial \eta}\frac{\partial y}{\partial \eta} \\ \frac{\partial x}{\partial \eta}\frac{\partial x}{\partial \xi} & \frac{\partial y}{\partial \eta}\frac{\partial y}{\partial \xi} & \frac{\partial x}{\partial \eta}\frac{\partial y}{\partial \xi} + \frac{\partial y}{\partial \eta}\frac{\partial x}{\partial \xi} \end{bmatrix} \tag{A4}$$

$$[J_2] = \begin{bmatrix} \frac{\partial^2 x}{\partial \xi^2} & \frac{\partial^2 y}{\partial \xi^2} \\ \frac{\partial^2 x}{\partial \eta^2} & \frac{\partial^2 y}{\partial \eta^2} \\ \frac{\partial^2 x}{\partial \eta \partial \xi} & \frac{\partial^2 y}{\partial \xi \partial \eta} \end{bmatrix} \tag{A5}$$

The matrices $[J_1]$ and $[J_2]$ are computed using equation (A2).

REFERENCES

1. J. N. Reddy, *Energy and Variational Methods in Applied Mechanics*, Wiley, New York, 1984.
2. J. N. Reddy, A generalization of two-dimensional theories of laminated composite plates', *Commun. Appl. Numer. Methods*, **3**, 173–180 (1987).
3. S. Srinivas, 'A refined analysis of composite laminates', *J. Sound Vib.*, **30**, 495–507 (1973).
4. H. Murakami, 'Laminated composite plate theories with improved inplane responses', *ASME Pressure Vessels and Piping Conference*, 1984, pp. 257–263.
5. R. L. Hinrichsen and A. N. Palazotto, 'The nonlinear finite element analysis of thick composite plates using a cubic spline function', *AIAA J.*, **24**, 1836–1842 (1986).
6. P. Seide, 'An improved approximate theory for the bending of laminated plates', *Mech. Today*, **5**, 451–465 (1980).
7. J. N. Reddy, E. J. Barbero and J. L. Teply, 'A generalized laminate theory for the analysis of composite laminates', *Report VPI-E-88.17*, Department of Engineering Science and Mechanics, Virginia Polytechnic Institute and State University, June 1988.
8. E. J. Barbero, J. N. Reddy and J. L. Teply, 'An accurate determination of stresses in laminated plates', *Int. j. numer. methods eng.*, to appear.
9. R. A. Chaudhuri, 'An approximate semi-analytical method for prediction of interlaminar shear stress in an arbitrarily laminated thick plate', *Comp. Struct.*, **25**, 627–636 (1987).
10. J. N. Reddy, *Applied Functional Analysis and Variational Methods in Engineering*, McGraw-Hill, New York, 1986.
11. N. J. Pagano, 'Exact solutions for composite laminates in cylindrical bending', *J. Compos. Mater.*, **3**, 398–411 (1969).
12. N. J. Pagano, 'Exact solutions for rectangular bidirectional composites and sandwich plates', *J. Compos. Mater.*, **4**, 20–35 (1970).
13. J. N. Reddy, 'A note on symmetry considerations in the transient response of unsymmetrically laminated anisotropic plates', *Int. j. numer. methods eng.*, **20**, 175–194 (1984).